SYNTHESIS REPORT

FOR PUBLICATION

CONTRACT N°: **BRE2-CT93-0524**

BE - 7010

TITLE: "Optimisation of design and performance of high damping rubber bearings for seismic and vibration isolation"

PROJECT COORDINATOR:

ENEL - **Società** per **Azioni**
D.S.R. - C.R.I.S.
Via **G.B.** Martini, 3
ITALIA -00198 ROMA

PARTNERS:

ALGA **S.p.A.**
ENEA
MRPRA
SHW
Dyckerhoff & Widmann AG
STIN S.p.A

STARTING DATE: 01.12.93 DURATION: **30** Months

Project funded by the European Commission under the **Brite/EuRam** II **Programme**

DATE: December 1996

STUDIES FOR THE OPTIMISATION OF DESIGN AND PERFORMANCE OF HIGH DAMPING RUBBER BEARINGS FOR SEISMIC ISOLATION

Franco Bettinali & Alberto Dusi
Hydraulic and Structural Research Center, ENEL S.p.A, Milano, Italy

Alessandro Martelli & Massimo Fomi
Energy Department, ENEA, Bologna, Italy

Giuseppe Bonacina
Structural Engineering Department, ISMES, Senate (Bergamo), Italy

Keith Fuller
TARRC (Tun Abdul Razak Research Center) former MRPRA, Hertford (United Kindom)

J.Eibl, K.H.Hehn
Institut fur Massivbau und Baustofftechnologie Universitat Karlsruhe, Karlsruhe (Germany)

Th.Baumann, W.Krause
Dyckerhoff & Widmann AG, Munchen (Germany)

Camillo Nuti
STIN, Roma (Italy)

Agostino Marioni
ALGA SpA, Milano (Italy)

Claudio Mazzieri
ANSALDO Ricerche srl, Geneva (Italy)

Claude Mortier
SHW Bruckentechnick GmbH, Esslingen (Germany)

ABSTRACT

Wide-ranging experimental and numerical studies have been carried out, in the framework of the BE7010 project funded by the European Commission, on High Damping natural Rubber Bearings (HDRBs) and structures which are seismically isolated by means of such bearings. This paper focuses on this project, which aimed at the optimisation of HDRBs for seismic and vibration isolation and at the evaluation of the technical and economic benefits of their use in the design of structures.
The activities and the main results obtained by the partners in the project are summarised and discussed.

1. INTRODUCTION

Traditional earthquake design methodology uses high strength or high ductility to mitigate seismic effects. An alternative approach consists in the isolation of the base of a structure from the ground by use of flexible devices, called isolators, placed between the superstructure and its foundations. A base-isolated structure is characterised by a quite low frequency, thus, during a strong earthquake, it moves like a rigid body over its isolation system. Deformations and energy dissipation are mostly concentrated in the isolators, Thus, a seismic isolator must be rigid in the vertical direction (to support the dead load of the superstructure), flexible in the horizontal plane (to allow for large relative displacements between the superstructures and the ground) and, possibly, it must be able to dissipate energy. HDRBs, which are composed by the superposition of steel plates and rubber layers bonded together, satisfy the above mentioned conditions (Forni et al., 1995 & Dusi et al., 1996). The early development and shaking-table evaluations culminated in their use in 1985 for the Foothill Communities Law and Justice Centre in California (Coveney et al, 1988). They are now among the most used isolators in the world and the only ones used in Italy (Martelli et al., 1996a). Their behaviour is mostly characterised by the rubber mechanical properties, which are quite non-linear. The horizontal stiffness is initially high, a fact which means the isolator provides intrinsic restraint against movement due to wind and earth tremors. The stiffness steadily decreases with rubber strain until in the range 50% to 100% - the usual range of response to design level earthquakes - it becomes practically constant. Finally, the stiffness increases up to the isolator failure, which can occur even over 400% shear strain (Dusi et al., 1996). The upturn at high strain maybe exploited to provide a gradually imposed restraint to very high horizontal displacements. The rubber damping is hysteretic, that is practically independent of velocity (some viscous effects are present but they can be neglected in most cases) but, like the stiffness, it vanes with the displacement.

The main purposes of the present project were to improve the quality and performance of HDRBs, to increase knowledge of their behaviour and to validate analytical methods used to produce the response of structures mounted on HDRBs. The work included:

* development of new higher damping rubber compounds;
* optimisation of design of bearings using finite element analysis;
* improvements in manufacturing techniques;
* consideration of installation, protection from hazards such as fire and maintenance during service;
* assessment of benefits of seismic isolations.

2. DEVELOPMENT OF COMPOUNDS

A key element in the first part of the project was the development at MRPRA of improved high damping compounds, a soft one with a shear modulus of 0.4MPa and a stiff one of modulus 0.8MPa. The main aim was to obtain a higher level of damping than that given by current compounds, particularly those with a low modulus. The target dynamic level was 12-15% of critical at 100% shear strain and a frequency of 0.5 Hz. Other properties for which improvement was sought were:

a) lower increase of shear modulus with decrease in temperature. For some existing compounds, the modulus is reported to increase by a factor of three as the temperature is lowered from 40°C to -20°C;
b) physical creep rate. It was realised that a low physical creep rate would, however, be difficult to achieve in conjunction with high damping;
c) change of modulus due to repeated cycling. The fact that the modulus of filled rubbers decreases under repeated cycling at a given strain slightly complicates prediction of the response of rubber seismic isolators. The reduction for existing compounds is typically well over 10°/0 between the first and sixth cycles;

In developing compounds with higher levels of damping, other properties had to be maintained at acceptable levels to ensure satisfactory performance of the bearings. The target minimum acceptable values included:

elongation at break %	600	
tensile strength MPa	14	
compression set % (7d @ 70°C)	45	
shear failure strain %	350	
G (40°C) / G(-20°C)	0.60	(G= shear modulus)

Selected properties of the two compounds developed are given in the following Table. In each case the damping is 3.5 percentage points above the levels previously attained; for the stiffer compound the level falls within the target range of 13-15%.

Compound	62	63
(*) Shear modulus	0.80	0.43
(*) Damping	13.8	11.5
Tensile strength MPa	19	18
Elongation at break%	570	780
Compression set %, 1d/70°C	40	38
Shear failure strain %	400	500
G (40°C) / G (-20°C)	0.56	0.56
($) Creep (% per decade)	17	19
Ageing 7d/70°C		
Hardness change (IRHD degrees)	+ 5	+ 4
Tensile strength % change	+3	+ 3 (^)
Elongation at break % change	-9	-9 (^)
(**) G (1st cycle) / G (6th cycle)	1.08	1.05
Low temperature hardness change (IRHD degrees) at -25°C after:		
6d	+ 15	+ 16
4d	+ 20	+ 36

Note:
1. (*) Dynamic test data for 0.5Hz, 100% strain 6th cycle.
2. Cure tot- at 140°C.
3. (^) Results for core at 120°C.
4. ($) Measured for shear deformation. Initial strain 50%.
5, (**) Test conditions 0.5 Hz, 100% strain.

The tensile strength, compression set and shear failure strain all meet the target values listed for both compounds. The shear failure strain in particular is high, though the value is likely to be influenced by the relatively low diameter/thickness ratio (4: 1) of the testpiece. The elongation at break for the stiffer compound is very slightly lower than the target 600%, but should give a reasonable larger ultimate shear displacement for the bearings. The other target that is not quite met is the ratio of the shear modulus at 40°C to that at -20°C. The increase in modulus at -20°C, even for the stiffer compound is, however, less than 10% higher than the target. It should be remembered that the modulus rise is accompanied by an increase in damping, thus reducing the net effect of temperature upon most aspects of isolation system performance. The physical creep rate (as measured in shear) is quite high, but should be perfectly acceptable for a bearing under vertical load. The change in modulus under repeated cycling, as quantified in the previous Table by the ratio of the first cycle to sixth cycle modulus, is quite low for a high damping rubber. The figures obtained, especial] y the 5% for the soft compound, achieve the objective of reducing design uncertainties due to this effect. The accelerated ageing data indicate behaviour similar to current high damping compounds.
The low temperature hardness results confirm the expectation, particularly for the soft compound, that these materials are susceptible to crystallisation during prolonged exposure to temperatures below -5°C. Little attention has been paid previously to the resistance of high damping NR compounds to low temperature crystallisation despite their greater susceptibility than conventional engineering compounds. Further development work has shown that blending the natural rubber with other elastomers can produce compounds with greatly improved crystallisation resistance whilst retaining other properties little changed.
One aspect of performance of the compounds that could not be fully assessed during the primary development stage was long-term anaerobic ageing. Assessment of the ageing behaviour of the compounds developed was earned out by experiments on rubber testpieces and bearings. The results are reported in section 4 and 5.

3. DESIGN AND PRODUCTION OF THE OPTIMISED HDRBs

A considerable number of HDRBs for the experimental campaigns at ISMES, ANSALDO-Ricerche and UNIKA and for the assessment of manufacturing technique were jointly produced by ALGA and SHW. These HDRBs are characterised by: (a) two rubber compounds, one harder (G = 0.8 MPa) and one softer (G = 0.4 MPa), which were developed by MRPRA (see §2); (b) various scales (diameter D equal to 125 mm, 250 mm, 500 mm and 800 mm); (c) two values of the primary shape factor, namely the ratio between the loaded and the unloaded areas of a single rubber layer (S = 12 and S = 24); (d) five different attachment systems (recess, bolts, central dowel, bolts & dowel, direct bonding).
Because experimental tests and finite element (FE) analyses on such isolators showed the possibility of further improving their stability at large deformations by decreasing their height, 30 "further optimised" and 12 "squatter" HDRBs were designed by ENEA and manufactured by ALGA. The heights have been decreased to 80?4 of the initial values for the "further optimised" HDRBs and 60% for the "squatter" HDRBs. The diameters were D 125 mm and D = 250 mm for the frost, and D = 250 mm for the latter. The attachment system was bolts & central dowel for the 125 mm diameter HDRBs, while recess has also been considered for the 250 mm diameter HDRBs.
For the optimisation of the fabrication process the following activities have been performed by ALGA: a) new moulds designed and built, b) new bonding agent tested, c) a new and better system for a layer thickness check developed and used in the fabrication process, d) all the different steps for rubber batches manufacturing checked and renewed (Rheo meter test, Shore hardness test and steel plate pre-heating), e) the vulcanisation cycle, for 500 and 800 mm diameter bearings, established, f) curing time determined, g) a better heat transmission in the vulcanisation process investigated by means of a new method (electrical induction, up to 140°C), the results was the reduction (70-80%) in the vulcanisation time and an uniform temperature distribution.

4. TESTS ON RUBBER SPECIMENS

4.1 General mechanical specimens

A comprehensive set of data has been obtained on the two compounds (64 and 65) used to mould bearings (see following Table).
The compounds differ very slightly in formulation from those (compounds 62 and 63) discussed in the compounds development section. The testpieces used were cured at 145°C, which is the temperature appropriate to the rubber near the outside of the bearings during moulding. Since the foundations are designed on the basis of a 120"C cure, the shear modulus (100% strain) of the compounds cured at 145°C would expected to be somewhat below the target figures of 0.8MPa and 0.4MPa.
The shear modulus of the harder compound is rather lower than expected, even allowing for the high cure temperature (145°C), from the data from compounds 62 and 63.

Compound	64	65
Shear modulus MPa (100%, 0.5Hz, 3rd cycle)	0.63	0.39
Damping % critical (100%, 0.5Hz, 3rd cycle)	16.0	12.5
Elongation at break %	620	720
Tensile strength MPa	17	17
Hardness IRHD	61	44
Change in hardness IRHD at -25°C after:		
6 h	+ 17	+ 22
22 h	+ 19	+ 23
4 h	+ 27	+ 30
Ageing 7d at 70°C:		
change in IRHD	+ 4	+ 3
% change in EB	-8	-3
% change in TS	0	+ 4
Shear failure strain % (testPiece 2 mm thick, 25 mm diameter)	485	575

4.2 Tests for the definition of the **hyperelastic model** of rubber

Stress-strain measurements on the two final compounds (64 and 65) in the unscragged state have been carried out at MRPRA in order to characterise the material adequately for FEA. Tests performed in uniaxial tension, uniaxial compression, simple shear, pure shear and bulk compression. The pure shear test-rig incorporated lateral load-cells so that the stress orthogonal to the displacement could also be measured. This has the advantage that $\partial W/\partial I_1$ and $\partial W/\partial I_2$ (W being the strain energy density and I_1 and I_2 the strain invariant) can be determined from one test. Experiments in pure shear with the lateral load-cell measurement confirm that $\partial W/\partial I_2$ is small compared with $\partial W/\partial I_1$ for values of (I_1-3) above 1.5 (shear strain of 120%) for compound 64, and (I_1-3) above 0.5 (shear strain 70%) for compound 65. The results for $\partial W/\partial 1_2$ also show that a larger strains it is virtually constant.

Though the Mooney-Rivlin series characterisation was used as input for the finite element analysis, additional study of the stress-strain data suggests that a Valanis-Landel type of energy function may be a useful alternative that in some respects fits the data better.

The bulk compression tests show a slight non-linearity in pressure-volume change behaviour. At about 4% strain the bulk modulus values determined were:

Compound	64	65
Bulk modulus GPa	2,55	2.38

In addition to experiments performed by MRPRA, tensile, compression, equi-biaxial, shear and compressibility tests on specimens of both the hard and the soft compound were performed by ENEL, with the co-operation of ENEA (Fig. 1). The aim was to define the data necessary for the implementation of the hyperelastic models of rubber, so as to enable FE calculations of HDRBs. Detailed guidelines for such tests were developed; specific equipment for equibiaxial and planar shear deformation tests was jointly designed and manufactured by ENEL and ENEA, which also jointly analysed the experimental data and defined the hyperelastic models of both rubber compounds.

4.3 Tests for the evaluation of temperature effects

The effects of temperature on the behaviour of specimens formed by both rubber compounds were evaluated by ANALDO-Ricerche (ARI), in addition to MRPRA, in a climatic chamber. The temperature range was from-20 “C to +4o ‘C. Some results for 100% rubber strain are summarised in the following Table. The average of the changes observed at the two laboratories are given.

Variation of modulus and damping with temperature				
Temp. 'C	Compound 64		Compound 65	
	G(T) / G(20)	d(T) / d(20)	G(T) / G(20)	d(T) / d(20)
40	0.89	0.90	0.89	0.90
20	1.00	1.00	1.00	1.00
0	0.32	1.09	1.22	1.05
-lo	1.48	1.16	1.40	1.15
-20	1.78	1.30	1.66	1.33

4.4 Tests for the evaluation of ageing effects

During service, the rubber in seismic isolators ages predominantly in an anaerobic manner. Thus to predict long-term performance of isolators from laboratory tests it is necessary to simulate anaerobic conditions. Another problem that must be avoided is the evaporation of volatile ingredients during high temperature ageing of small testpieces.
Experiments *using* testpieces (wrapped with metal adhesive tape to simulate anaerobic conditions) to assess the changes in dynamic properties during ageing gave changes in modulus much larger than the changes in stiffness observed during ageing of bearings.
Bearings (fabricated from compound 64) increased in stiffness by only 10% under quite severe ageing conditions (8 months at 70°C). It thus appears that further work is needed to develop a suitable equivalent of anaerobic conditions for small dynamic testpieces.
Tests were also performed on artificially aged rubber specimens, in order to verify the possibility to develop and implement hyperelastic models of the aged rubbers in FE models of HDRBs. In fact, the demonstration that the ageing effects on HDRBs can be forecasted analytically based on the results of tests on specimens is quite an important results, because it permits to only age and test rubber specimens, thus saving the non-negligible costs of tests on the entire aged HDRBs. To this aim, ANSALDO-Ricerche aged specimens provided by ALGA using the same procedure as adopted by UNIKA for the entire isolators (4 months at 70 "C), ENEL tested them and, in co-operation with ENEA, analysed the test data and implemented them in the hyperelastic model of the rubber.

4.5 Other rubber tests

Cavitation

A negative hydrostatic pressure of the order of the shear *modulus* causes rubber to cavitate. For seismic isolators this phenomenon is important in two circumstances. First, when the isolators is bolted to a structure and sufficient uplift occurs to subject the isolator to a significant tensile force, and secondly at large shear deformations because tilting of the end reinforcing plates subjects part of the end rubber layers to tensile forces.
The cavitation stress for compounds 64 and 65 has been estimated by pulling rubber discs in tension. The results from discs of shape factor (= radius/ (2 x thickness)) in the range 9 for 20 were similar:

Compound	64	65
Cavitation stress MPa	3.4	2.5

Despite the occurrence of cavitation at modest stresses and strains, ultimate tensile failure of the discs typically occurred at stresses about three times the cavitation stress and strains of the over ten times the cavitation strain.

Cycling and strain-history effects

Cycling and strain history effects may be important in determining the response of isolators to earthquake inputs. In particular, a large displacement will soften the isolators. At least partial recovery towards the original properties is expected.
Detailed tests (see following Table) to look at the first quarter cycle of loading have been earned out, and a secant modulus calculated. The software used to analyse the for dynamic data considers the first cycle to start after 3/4 cycle. It is apparent that much the largest change occurs due to the first 3/4 cycle.

Compound		64	65
Secant shear modulus G (MPa) at 100% strain		0.93	0.50
Dynamic shear modulus (MPa) at 100?'o	1st cycle	0.76	0.43
	6th cycle	0.68	0.40

An assessment of strain history effects on dynamic properties has been carried out. The effect of an orthogonal 200% or 300% shear strain on 100% *strain* modulus is given below:

	Compound	virgin	Time after pre-strain			
			200%		300%	
			2 min	74 hr	2 min	74 hr
Dynamic shear modulus MPa (6th cycle, 100% strain 0.5 Hz)	64	0.40	0.35	0.39	0.33	0.37
	65	0.68	0.56	0.62	0.51	0.59

It is clear that a large strain orthogonal to the smaller strain test direction produces a substantial softening effect. Over a time stale of three days the rubber has recovered about 50% of the change, though for the soft compound 65 the recovery is almost complete after three daYs. The effects of 200% and 300% shear pre-strain on the modulus at 100°/0 strain (applied in the direction of the pre-strain) is shown below for compound 64:

	virgin	Time after pre-strain			
		200%		300'%0	
		2min	116 hr	2min	116 hr
Dynamic shear modulus MPa (6th cycle, 100% strain 0.5 Hz)	0.70	0,55	0.62	0.50	0.58

The magnitude of the changes is very similar to those seen following a large pre-strain applied orthogonal to the 100% test strain. About half the change is recovered over 5 days: .the recovery occurs approximately logarithmically with time.

5. TESTS ON THE INDIVIDUAL HDRBs

The activities on this topic have concerned the execution of experiments on both non-aged (virgin) and artificially aged HDRBs. As far as the tests on non-aged HDRBs are concerned, tests were performed, (1) at room temperature at ISMES and the Nuclear Engineering Laboratory (LIN) of the University of Bologna (ENEA tests), and (2) at various temperatures at ARI (ALGA tests). In order to optimise test quality ENEA significantly improved SISTEM (Seismic ISolation TEst Machine), which is located at ISMES, and designed and manufactured a second equipment (CAT - Creep and Ageing Test) for long duration creep tests, which was installed at LIN.

5.1 Tests at ISMES of the initially developed isolators

The ISMES experiments on the initially developed HDRBs were completed, by means of SISTEM. They concerned several HDRBs with two different scales, both S values, both G values and Up to the five different attachment systems (AS) which were previously mentioned, namely: (a) 10 isolators with D = 250 mm, S = 12, G = 0.8 MPa, 4 ASS; (b) 16 isolators with D = 250 mm, S = 24, G = 0.8 MPa, 5 ASS; (c) 4 isolators with D = 250 mm, S = 12, G = 0.4 MPa, AS= bolts and central dowel (BD); (d) 4 isolators with D = 250 mm, S = 24, G = 0.4 MPa, AS = BD; (e) 4 isolators with D = 500 mm, S = 12, G = 0.8 *MTa,* AS = BD. These experiments comprised:

(a) quasi-static vertical compression tests (loading velocity = 5 kN/s) for the evaluation of vertical stiffness;
(b) quasi-static shear tests (loading velocity = 50 mm/min) under constant vertical compression load (V) for the evaluation of static horizontal stiffness at 50%, 100% and 200% shear strain (ratio between the horizontal displacement and total rubber height);
(c) quasi-static shear tests at 100% shear strain with different vertical compression loads (from 0.25 V to 2 V) for evaluating the effects of vertical load variation on horizontal stiffness;
(d) dynamic shear tests at various frequencies (O. 1,0.4, and 0.6 Hz), under constant V and at various shear strain values (from 10% to 200%), to evaluate the equivalent viscous damping and dynamic effects on the horizontal stiffness;
(e) some sustained compression tests for evaluating creep effects;
(f) quasi-static failure tests due to compression and shear.

ENEA and ISMES analysed part of the very numerous test data, by confirming the fulfilment of the target values for several parameters, in particular that:

(1) the behaviour of all the considered attachment systems is excellent and practically equivalent to 200% shear strain (Fig. 2);
(2) the behaviour of the optimised HDRBs with attachment systems consisting in bolts, bolts and central dowel and direct bonding is good to the target value of 300% shear strain at least (Fig. 3);
{3) the equivalent viscous damping ratio is well larger than the target value of 10% for both compounds considered (Fig, 4);
(4) the dependence of horizontal stiffness on frequency is limited, as desired (Fig. 5);
(5) the performance of HDRBs can be further improved by modifying the secondary shape factor, namely the ratio between the loaded and the unloaded areas of the entire isolator.

5.2 Tests at **ISMES** of 'further optimised' isolators

In January 1996, tests were also completed at ISMES on 12 'further optimised' HDRBs; these have D = 125 mm, S = 12, G = 0.4 MPa and the attachment system formed by the combination of central dowel and bolts (BD). Six of them are those being used (February 1996) in the shake table tests on an isolated structure mock-up, which are described later: in order to characterise them correctly (so as to enable a reliable analysis of the shake table tests), these HDRBs were subjected to both quasi-static vertical compression tests at the design vertical load V = 50 kN, and quasi-static cycling shear tests where the lateral displacement was gradually increased up to 200% shear strain under constant V (Fig. 5-his}.

As regards the remaining six HDRBs the following tests were performed:

(a) quasi-static vertical compression tests (loading velocity = 5 kN/s) of 6 isolators up to 3V = 150 kN;
(b) quasi-static test (loading velocity = 50 mm/min) of 1 isolator where the horizontal displacement was cycled up to approximately 250% shear strain at constant vertical load equal to 2V = 100 kN (Fig. 6);
(c) quasi-static vertical compression tests (loading velocity = 10 Id'J/s) of 1 isolator for the evaluation of vertical stiffness at various values of the vertical load, where the latter was increased to 670 kN (i.e. more than 13 V - see Fig. 7), then it was discharged and was failed by subjecting it to a rather large tensile load of 40 kN (i.e. to -0.8 V);
(d) dynamic cycling shear tests of 1 isolator under constant V at f = 0.1 Hz, 0.4 Hz, 0.6 Hz and 0.8 Hz, where the horizontal displacement was gradually increased to 200% shear strain;
(e) dynamic cycling shear test of the same isolator as in step (d) under constant V at f = 0.1 Hz, where the lateral displacement was gradually increased to failure (Fig. 8);
(f) quasi-static shear test Of 1 isolator under constant V, where the lateral displacement was gradually increased to failure (Fig. 9),
(g) quasi-static shear test (loading velocity =50 mm/min) of the isolator that had failed in test (f) to 200% shear strain (Fig. 10).

As regards such tests and their results the following remarks are worthy

- Tests (c) showed that the safety factor for the vertical load is quite larger than the value 3 that is required, for instance, by Forni et al. (1994) for the SI of nuclear plants and that the rubber and bonding quality are excellent.
- The conditions of tests (a) and (b) (where no fixability problem was detected) were considerably more severe than those required by Fomi et al. (1994), in addition to that mentioned above, in the case of bolted bearings (200°/0 shear strain at V; 170% shear strain at 1.7 V).
- Due to the small sizes of the considered isolators (thus, the small value of V) considerable problems were found for the control of vertical load in tests (d) for frequencies larger than 0.1 Hz; this is the reason why test (e) was performed at f = O. I Hz.
- However, control of vertical load was again poor in test (e) at large shear strain, even with f = 0.1 Hz: in particular, the *isolator was* subjected to 4V (200 kN) when it failed at 450% shear strain.
- Thus, in order to correctly determine the shear strain value at which the isolators fail (namely, by really keeping V constant), test (f) was performed; the results of this test show that failure occurs at approximately 400% shear strain, which is in good agreement with the pre-test analysis of Fomi et al. [1995): this value is somewhat lower than that of test (e), where, however, the poor control of vertical load might explain the discrepancy.
- Finally, the results of test (g) on the broken isolator are consistent with those of experiments performed in other laboratories (for instance at Earthquake Engineering Research Centre, University of California at Berkeley), by showing that even severe damage of rubber bearings does not lead to lack of support of the superstructure up to a rather large shear strain (Fig. 10).

5.3 Remarks on tests at **UNIKA**

The 800 mm diameter initially developed HDRBs (together with part of the 500 nun diameter bearings and some 250 mm diameter bearings) were tested by UNIKA, using the same experimental procedures as ISMES. Similar tests were also carried out *by UNIKA on virgin and* aged *250 mm* diameter 'further optimised and 'squatter' HDRBs. The experiments comprised:

(a) compression tests under vertical load; the compression stiffness K_v, evaluated as secant modulus in the 3rd cycle of a quasi static load, has been compared with the one given by the following formula:
$K_v = 66GS(A/T)$ (with G modulus of elasticity, S shape factor, A area and T total rubber height). In the case of aged isolator (4 and 8 months) a 7% increase has been recorded.
(b) compression-shear combined tests; (1) quasi static tests (at 50%, 100% and 200% shear strain} have shown a 5% to 11% increase in horizontal stiffness in a 4 months aged bearing with a media of 10% in all the tests at different shear strain and a negiglible difference, between bolted and unbolted isolators, within 200% shear strain; (2) dynamic tests (100% and 200°/0, 0. 1Hz at vertical design load) have shown a decrease in the horizontal stiffness due to a "scragging effect" cause by the pre-loading phase;
(c) quasi static shear failure tests; (only on a 250 mm diameter isolator); (1) for bolted isolator at the end of a continuous force increase, the shear failure, occurred when the eccentricity of the applied vertical load reaches the outer edge of the compressed

isolator side, was induce by a Successive tearing of the tension zone within the rubber layer followed by a complete shearing of the remaining cross section (a total shear failure, at about 380%, was preceded by a pronounced tilting of the inner steel); (2) for recess connection after an end plates lift off at tensile sides and a "roll out" movement, failure in reached after the isolator end plate contacts the connection plate on the opposite side giving rise to an increment in the shear force for a value of 460°/0 shear strain.
(d) effect of ageing; for aged bolted bearings an increase of failure load (+40%) and a decrease of shear at failure (-10% with respect to the virgin one) was detected.

5.4 **Vertical compression and creep tests at LIN**

Experiments were also earned out at LIN on CAT (Fig.11) for the four 500 mm diameter HDRBs that were tested at ISMES; at first they consisted in a characterisation under vertical compression loads (to compare the results to those obtained at ISMES on SISTEM), then (simultaneously for all isolators) in the beginning of a creep test under V = 1,600 **kN,** which will last six months.

5.5 **Evaluation of temperature and ageing effects at ARI**

As regards the evaluation of temperature effects, ARI completed the ALGA tests on the virgin initially developed bearings with D = 125 mm and the attachment system formed by bolts and central dowel, for the harder rubber, and is performing those on the softer rubber bearings. These tests have been and are being carried out on pairs of the HDRBs in a climatic chamber; temperatures range from -20 °C to +40 'C, similar to the robber specimens.
ARI also performed tests on aged 125 mm diameter HDRBs (for both compounds), so as to allow for comparisons with the results of tests performed on aged rubber specimens. Isolators were some of those initially manufactured for the shake table tests (i.e. not those 'further optimised). Since it was not advisable to use the HDRBs which have already been tested at ISMES in virgin conditions (too many tests were performed, even at low and high temperatures), some of the new bearings were characterised before ageing, so as to clearly identify the ageing effects. Isolators were aged by ARI using the same procedure as at UNIKA (4 months at 70 'C, similar to the rubber specimens). Afterwards, ARI tested them both at room temperature and in the climatic chamber: in this way it will be possible to also evaluate the combined effects of temperature and ageing. This activity was complementary to that to be performed by UNIKA on the 'further optimised 250 mm diameter HDRBs.

5.6 **Structural detailing of HDRBs**

Stability, integrity ad load bearing capacity under service and emergency conditions have been investigated at Dyckerhof & Widmann. Tests reproducing accidents conditions as high temperature and fire, extreme low temperature caused by a leaked liquefied gas and chemical attacks by inorganic liquids, organic fluids and gases have been carried out on full-scale isolators. These experiments comprised:
(1) heat radiation and fire resistance test under vertical load, (non-protected devices under heat radiation and fire, protected device under fire). While fire resistance tests on a 500mm diameter devices under a 1570kN vertical load without any fire protection have shown that stability and load bearing capacity is maintained for 45 minutes only, the same device with a rock wool boards fire protection has performed well for 3 hours.
(2) cryogenic temperature tests. A non-protected 250mm diameter devices under a vertical load of 400kN was subjected to a cryogenic temperature of - 196°C up to the complete freezing. A decrease in the vertical and horizontal stiffness (-20%) was recorded. The vertical load was substained for the whole test demonstrating the device ability to withstand successfully such kind of attack. The device was replaced after test (cracks induced by a bond deterioration between rubber and steel plate were recorded). A new replacement method was developed during the project. The method, applicable when it is not possible to jack up the building resting on bearings, implies, after having removed the devices, to destroy the mortar bed by means of an high pressure water jet (1000 bars), and to install a new bearing, loaded by a flat jack filled up with cement grout. Test was successful and the applicability of the proposed procedure clearly demonstrated.

6. **TESTS ON ISOLATED STRUCTURE MOCK-UPS**

In the framework of BE701O project, two isolated structure mock-ups are being tested: the first, with a flexible superstructure (MISS), was subjected to shake table tests, while the second, with a rigid superstructure, was subjected to free-vibration tests. In addition, as mentioned by Martelli et al. (1996a), the use of some HDRBs developed in this project has been planned for pseudodynamic tests on large scale isolated structures at the Joint Research Centre of Ispra of the EC, in the framework of the Seismic Isolation Project of Renda et al. (1996).

6.1 Shake table tests **of the MISS mock-up**

The MISS (Model of Isolated Steel Structure) structure mock-up was manufactured for shake table tests at ISMES. It was jointly designed by ENEL, ENEA and ISMES. MISS is a four storey steel frame, to be supported by four or six 125 mm diameter HDRBs and provided with movable masses on each storey and variable interstorey distance, so as to allow for different stiffness, mass profiles and eccentricities. In the ISMES tests the six previously mentioned 'further optimised soft HDRBs were installed at the base of MISS.
ENEA and ENEL provided support for the design of the experiments. To this aim, FEMs of the entire MISS (see Fig. 12) and some critical parts (foot) were implemented in ABAQUS. By means of these models the maximum acceleration and displacement values that are admissible during tests were computed; in addition, natural frequencies of MISS were calculated

for different assemblages, including eccentric configurations. The results showed that it will be possible to achieve significantly low isolation ratios and to reach shear strain values of the isolators which are larger than 200%.
The MISS mock-up tests are being performed by applying one-directional (1D), 2D and 3D simultaneous excitations corresponding to real earthquake records in various soil conditions.

6.2 Free-vibration tests of a rigid superstructure mock-up
Pull-back tests of ALGA were performed at ARI on a 1,600 kN rigid mass isolated mock-up, supported by four 250 mm diameter 'further *optimised'* HDRBs. Such *tests* were limited to *the* harder rubber compound, with combined bolt and dowel attachment system: the reasons are both that the softer HDRBs will be used in the ISMES tests on MISS and that the vertical compression load as applied by the rigid mock-up would be too large for the soft bearings. The initial displacement in the pull-back tests were gradually increased Up to the maximum value compatible with the used jack.

7. SIMPLIFIED NUMERICAL MODELS OF THE HDRBs

The definition of simplified numerical models of the HDRBs, based on the results of single bearing tests, is necessary for the analysis of isolated structures (Martelli *et al.,* 1996a). Such models, however, shall be capable of accounting for non-linear horizontal stiffness and the hysteretic nature of damping. To this purpose ENEA completed the setting-up of an improved version of its computer program ISOLAE for the simplified analysis of S1 systems (Martelli *et al.*, 1995).

However, the development of a new simplified model of the HDRBs that can be directly implemented in ABAQUS also began at ENEA and ENEL. This consists of a combination of a non-linear spring with an elastic-plastic beam (Fig. 13-a, 13-b). By appropriately defining the physical parameters of the system (spring stiffness, Young's modulus and yield point of the beam) it is easy to reproduce the hysteresis cycle of a HDRB, including hardening and/or yielding and hysteretic nature of damping. Work has been performed by ENEL to define some identification criteria and by ENEA for the pre-test calculations of shake table experiments at ISMES. This was used by ENEA, ENEL and UNIKA in the analyses of isolated structures.

8. DETAILED NUMERICAL MODELS OF THE HDRBs

ENEA and ENEL jointly implemented the HE models of both rubber compounds in ABAQUS, based on the results of the specimen tests performed by ENEL. Non-linear models of the HDRBs were developed for both shape factors considered and for the various attachment system types. The need for including rubber compressibility effects in the HE model (thus, for specific tests *on* rubber specimens) was detected (Fig. 14).
The FEM of the initially developed isolators were defined and validated based on the results of the related single bearings tests (Forni *et al.*, 1995). Detailed HDRB models were also developed for the 'further optimised and 'squatter' HDRBs (Fig. 15). Pre-test calculations were performed for such bearings to 400% and 500% shear strain, respectively. The results will be compared to those of ISMES and UNIKA tests.
Finally, the HE models of aged rubbers will be developed based on the results of the specimens tests at ARI. These models will be implemented in the isolators' FEMs, which will be used to analyse the results of tests of ARI and UNIKA on the entire aged HDRBs.

8.1. Finite Element Modelling at ENEA/ENEL

The behaviour of the bearings under vertical load and shear strain has been modelled by means of finite element analyses, performed using the ABAQUS code, version 5.5 (ABAQUS, 1995).

8.1.1 Material models

The mechanical behaviour of rubber-like materials is described in ABAQUS by means of an elastic, isotropic and approximately incompressible model. The governing constitutive equations are derived assuming the following polynomial form (Rebelo, 1991) for the strain energy fiction U

$$U = \sum_{i+j=1}^{N} C_{ij}\left(\bar{I}_1 - 3\right)^i \left(\bar{I}_2 - 3\right)^j + \sum_{i=1}^{N} \frac{1}{D_i}\left(J_{el} - 1\right)^{2i} \qquad (1)$$

being $\bar{I}_1$ and $\bar{I}_2$ the first and the second invariant of the deviatoric strain, J the elastic volume ratio, C_{ij} and D_i material constants and N the order of the energy function. The value of the constants D_i determines the compressibility of the material and is set equal to zero for fully incompressible materials. The choice of N (generally N = 1, 2, 3) provides polynomial forms of strain energy more or less complex.
The coefficients in (1) can be defined by the data of experimental *tests involving simple* state of deformations and stress. Uniaxial, biaxial and shear experiments were used (Ogden, 1984; Rebelo, 1991 and Forni et al., 1995) to determine the above mentioned constants. For all the different compounds analysed in this study, the characterisation tests on rubber specimens have been carried out at ENEL-CRIS Laboratories (Bettinali et al., *1996).* In the numerical analyses reported in "this paper the material was assumed to be incompressible ($D_i = 0$) when studying shear deformations and a polynomial N =2 form was adopted.
As regards the steel shims, an elastic-plastic constitutive behaviour was assumed.

8.1.2 FE discretization

The difficulties encountered dealing with the incompressibility of rubber-like materials were treated by means of a mixed FE formulation. Hybrid elements have been used; in these elements the pressure stress is independently interpolated from the displacement field, making the numerical formulation of the variational problem well-behaved. An updated Lagrangian formulation is adopted.

Analyses carried out using several kinds of FE models showed (Dusi et al., 1995 and Forni et al., 1995) that rubber layers can be successfully modelled with eight-node elements (C3D8H - ABAQUS Manuals, 1995), which provide linear displacement and constant pressure interpolations, and steel plates with eight-node elements using reduced integration and linear displacement (C3D8R).

At least 8 subdivisions along the radius, 32 subdivisions along the external circumference were employed in the meshing; each rubber layer had three C3D8H elements through its thickness while each steel shim had only one C3D8R element through the thickness.

When modelling the recessed bearings, better results have been obtained using hybrid triangular elements (C3D6H), with six nodes, linear displacement and constant pressure, placed at the inner and outer borders of the bearing.

Pre-processing of the geometry, boundary conditions, materials properties and loads were undertaken using GENESIS (Dusi, 1996), a pre-processor for ABAQUS, which is capable of automatically generating the rather complicated ABAQUS input file on the basis of a few input data.

The geometry of the devices and the loading conditions make the problem symmetric. Therefore only one half of the bearing is usually modelled (figure 16-a), by imposing appropriate boundary conditions on displacements and rotations of the nodes belonging to the plane of symmetry The problem is also hemi-symmetric with respect to the plane parallel to the bases of the device and containing its centre of mass. In this paper the authors are therefore proposing the modelling of only a quarter of the device to be analysed (figure 16-b). Deformations of the HDRBs considered in this work pointed out that a further hemi-symmetry condition can be taken into account in the FE modelling of these devices. An hemi-symmetry about the straight line lying in the hemi-symmetry plane and perpendicular to it exists. Hence, appropriate constraints are invoked along the line of symmetry. In spite of a significant reduction of computational effort required to run the 3 D models, the comparison between the results obtained following this approach and those obtained from the modelling of half a bearing, shows that the considered FE models are equivalent from the global response point of view, as shown by figure 16-c.

8.1.3 FE analyses

Appropriate boundary constraints were applied to the models to simulate the actual service conditions: each bearing was first compressed with the relevant compressive load, then sheared by keeping the vertical force constant until the target value of shear strain was reached.

In order to reproduce the experimental conditions of the bolted device, the FE models assume that the top and bottom faces of the bearings are constrained to remain parallel. While the base plate nodes are fully constrained, every node of the top plate is tied, by means of constraint equations, to a pilot node located at the centre of the device; either the vertical and the horizontal loads are then applied to this pilot node.

The recess attachment system is more difficult to be modelled because it involves sliding of a deformable body (the bearing) against a rigid body (the recess plate). In this work, the contact problem was solved by meshing the recess plate' surface using rigid surface elements (IRS4).

.8.2 Finite Element analyses: results and discussion at ENEA/ENEL

8.2.1 Optimised HDRBs

The actual experimental test on the 1:2 scale bolted bearing, having a shape factor of 24, subjected to a vertical load of 400 kN (in the case of harder compound) and a horizontal displacement of 225 mm, namely 300% shear strain, is shown in figure 17-a, while in figure 17-b the deformed FE mesh is reported. The 3D numerical model provides deformation and values of stiffness well matching the experimental data (figure 17-c).

Figures 18-a, b, c and 19-a, b, c show the results obtained for 1:2 scale bearings with recess attachment system, respectively for a S=24 device, subjected to a vertical load of 40 t and to 200% shear strain, and for a S= 12 bearing under 40 t of vertical load and 3000/0 shear strain.

The deformed configurations provided by the FE models, shown in figures 18-b and 19-b, simulate the actual behaviour of the device well. In both cases the agreement between numerical and experimental horizontal stiffness is good.

8.2.2 Further optimised HDRBs

A comparison between the experimental data and the deformed mesh for the 1:4 scale bolted bearing, subjected to a vertical load of 50 kN and a horizontal displacement of 120 mm, namely 400% shear strain, is reported in figures 20-a and 20-b.

The agreement between numerical and experimental results is quite good. It has however to be observed that, at high shear deformations, the simulated response exhibits a lower shear stiffness with respect to the experimental one. This is probably due to the hyperelastic model implemented for this compound. The coefficients for the polynomial form of the strain energy function (1) were defined from shear tests performed on rather narrow specimens: in these conditions boundary effects could become significant at shear strain higher than 200%, thus leading to a softer behaviour.

8.3 Material models and FE analysis at UNIKA

Shear tests on elastomeric bearings Up to failure (400% shear strain) have been numerically performed with ABAQUS, assuming different constitutive law for rubber:

8.3.1 Ogden hyperelastic constitutive law (incorporating volumetric compressibility)

Constitutive law material parameters were obtained from tests performed by UNIKA in the past on testpieces, compared with the one obtained by ENEL and, after theoretical considerations, the same have been extended to a 3 dimensional domain, In this way it was possible to tit, in a qualitative and quantitative manner, the laboratory results even when instabilities (roll-out and snap-through) occur at around 400% shear strain {of course the hysteretic loop is not reproduced).

These analyses have clearly shown that for a more complete simulation of bearing performance a improved consistent triaxial constitutive law is necessary.

8.3.2) Viscolelastic Simo model

The basic assumption of the chosen law (Simo) are: 1) uncoupled volumetric and deviatoric response for finite strains, 2) viscoelastic properties approximated by a standard linear solid and 3) no volumetric relaxation.

In the strain energy function, completely defined with 7 parameters, the first term covers the volumetric stress (1 parameter) and the second one the deviatoric part; the last is described by a convolution integral depending by a) relaxation function (exponential G modulus variation in time, defined with 3 parameters: G at short time, G at infinite time and relaxation time), b) a strain softening damage function (defined with 2 additional material parameters) and c) a strain hardening function (defined another material parameter). After having verified the constitutive law with one element shear and tension tests the foilowing FE analysis have been performed:

1) ASTM tests:

On an ASTM-specimen, represented with 20-node quadratic continuum elements, a simulation of static and dynamic load histories have been performed and after the evaluation of the convolution integral the comparison between the laboratory and numerical hysteresis loop confirmed the ability of the law to correctly describe the rubber behaviour. The best fitting was obtained for high cycle, with respect to the lower one, because the relaxiation time was originally assume as the one obtained at 200% shear strain.

2) Bearings

In FE models of the bearings [20-node quadratic continuum elements for the rubber layers and the two ending steel plates, 8-node double curved shell elements for the reinforcement steel layers) the steel parts have been considered behave linearly. Two bolted bearings (250 nun diameter, 45 and 75mm total rubber thickness) have been considered and the static and dynamic test reproduced numerically. The very low discrepancy between laboratory and computation (3% in damping for a 150-200°/0 shear strain) has demonstrated that is possible to correctly evaluate the bearings behaviour assuming the same law derived by the test on ASTM testpieces. Due to the influence on the numerical results of the relaxation time special care needs to be paid to the range in which it has been evaluated.

9. EVALUATION OF BENEFITS OF SEISMIC ISOLATION

ENEA and ENEL are contributing to the evaluation of benefits of SI through the analysis of the isolated buildings of the Centre of the National Telephone Company (TELECOM Italia) at Ancona and the twin isolated and conventionally founded apartment houses at Squillace (Calabria), for which detailed experimental results from on-site tests are available to them in various locations, axial positions and directions (Martelli and Castoldi, 1991, Fomi *et* al., 1993). In all these buildings HDRBs have been used.

A new 3D FEM of the TELECOM building that had been subjected to on-site tests was developed by ENEA. This is much more detailed than those developed in the design analysis and pre-test calculations performed in 1990 (Fig. 21). The purpose was also to permit a very complete comparison between the numerical results and the quite numerous test data. For the calculations related to large displacements, ENEA used the simplified HDRB model described above. On the contrary, for the small excitations, a linear isolator model will be sufficient. The model is being validated by means of 3D calculations using both the data measured on the building during forced excitation tests with a mechanical vibrator on the roof and those measured during the pull-back tests. The first results, which corresponded to small amplitude excitations, will mainly allow for the validation of the superstructure model (deformation modes), while the latter, which corresponded to displacements up to I IO mm (i.e. close to the design value of 140 mm) will allow for the validation of the complete isolated model.

Also as regards the Squillace houses, both of which were tested by means of a mechanical vibrator installed on their roof, previous FEMs and validation analyses are being considerably refined and finalised by ENEL. After validation of all the above-mentioned FEMs, the benefits of SI will be identified by ENEA and ENEL by applying one-directional (1D), 2D and 3D actual seismic records on various soil conditions, corresponding to actual earthquakes (e.g. Tolmezzo records on medium soil of the 1976 Friuli earthquake, Calitri records on relatively soft soil of the 1980 Campano-Lucano earthquake, etc.), to the FEMs of the completed buildings. Such calculations will be performed for various values of the isolation ratio, from the actual isolated building to the conventional fixed base building.

Dyckerhoff & Widmann contributed to the evacuation of benefits of SI through the analysis of a LNG (Liquefied Natural Gas) tank system (an inner steel tank and an outer concrete one). It has been verified in different numerical analysis that the insertion of a base isolation system causes 1) an increment of the fundamental period of the inner tank, the most critical part, from 0.3 sec up to 2.0/ 3.5 sec and 2) a decrement in the seismic effects, also verified for different soil conditions, peak ground

accelerations and isolator stiffness, of about 20% (the "elephant footing" failure mode: the tank buckling caused by overturning moments can be, in this way, more easily prevented). An additional reduction in seismic forces, has been obtained thanks to the high hysteretic damping of the developed bearings.
In addition, the excitation in the horizontal and vertical direction acting simultaneously and the one with an horizontal direction only gave the same results, at least in term of hoop forces in the steel tank wall (reference forces usuall y assumed in the design). It has been observed that, even the vertical seismic components has a not negligible influence on the inner tank sliding, the isolation system contributes in the reduction of the effects of this movements.

10. CONCLUSIONS

The studies described above are considerably extending the knowledge previously acquired on the behaviour of HDRBs and will make optimised isolators available at reasonable costs. The so far obtained results, according to the project goals, confirm the capability of SI of considerably enhancing the seismic protection of civil and industrial structures, including nuclear plants. They have also provided important input for the development of the standards for seismic isolators and design guidelines for isolated structures that have been mentioned by Martelli et al. (1996a).

11. ACKNOWLEDGEMENT

This work has been supported by the European Commission, Directorate General for Science, Research and Development, Bnte EuRam II programme, Project BE-7010 Contractn.BR2-CT93-0524. All the partners wish to thanks Madam H.Laval of the Directorate General for Science, Research and Development of the European Commission for the continuous and fruitful support given during all the project life.

12. REFERENCES

ABAQUS Manuals, 1995, Version 5.5, Hibbitt, Karlsson & Sorensen Inc., Providence, Rhode Island, USA.

Bettinali F., Cazzuffi D., Dusi A., Fede L., 1996, *Valutazione delle Caratteristiche di Mescole in Gomma Naturale Utilizzate per la Costruzione di Isolatori Sismici,* ENEL S.p.A.-CRIS internal report n° 5187, (in italian).

Coveney, V.A., Derham, C.J., Fuller K.N.G., and Thomas, A.G., 1988, *Vibration isolation and Earthquake Protection of Buildings, in* Rubber Sci. & Technol. (Roberts A.D., Ed.) OUP

Dusi A., Fomi M., 1995, *FE* Models *of Steel Laminated Rubber Bearings,* Proc. 6th National Congress of ABAQUS Users' Group Italia, Bologna, Italy.

Dusi A., 1996, *GENESIS: a Pre-processor for the Implementation of 3D FE Models of Seismic Isolators,* ENEL S.p.A.-CRIS internal report n" 5283.

Dusi, A., Fomi, M,. La Grotteria, M., Sobrero, E., Zanotelli, G. L., 1996, *Behaviour of seismic isolators at very large shear strain,* Proc. ABAQUS Users' Conference, Newport, RI, USA.

M. Forni, A. Martelli, L. Grassi, E. Sobrero, F. Vestroni, F. Bettinali, G. Bonacina, E. Pizzigalli, 1993, *Analysis of in-situ forced vibration tests of twin isolated and non-isolated buildings,* Proc. of the 1993 ASME-PVP Conference, Denver, Colorado, USA, PVP-Vol. 256-2, Y.K. Tang Ed., ASME, New York, pp 217-229.

Fomi, M., Martelli, A. Cesari, G. F., Di Pasquale, G., Marioni, A., and Olivieri, M., 1994, *"Proposal for Design Guidelines for Seismically Isolated Nuclear Plants",* Find Report, EC-ENEA Contract ETNU-003 l-IT, EC, Bruxelles, Belgium; EC Report in press.

Fomi, M., Martelli, A., Bettinali, F., Dusi, A., Castellano, G., 1995, *Hyperelastic models of steel-laminated rubber bearings for the seismic isolation of civil buildings and industrial plants,* Proc. ABAQUS Users' Conference, Paris, France, pp 273-287.

Martelli, A. and A. Castoldi, 1991. Seismic isolation of structures. In: *Experimental and* Numerical *Methods in Seismic Engineering* (J. Donea and P.M. Jones, Eds., Kluwer Academic PubIs.), pp. 351-377.

Martelli, A., M. Fomi, B. Spadoni, A. Marioni, C. Mazzieri, F. Bettinali, G. Bonacina, G. Pucci, F. Cesari and E. Sobrero (1995). *Progress in applications and experimental studies for isolated structures in Italy. In:* Proc. Int. Post-SMiRT Conf. Seminar on Seismic Isolation, Passive Energy Dissipation and Active Control of Structures, Santiago, Chile (R. Saragoni, Ed.).

Martelli, A., Forni, M., Bettinali, F., Marioni, A., Bonacina, G., 1996a, *Overview on the progress of Italian activities for the application of seismic isolation,* Proc. of the 1996 ASME-PVP Conference, Montreal, Quebec, Canada, July21 -26.

Ogden, R. W., 1984, *Non-Linear Elastic Deformations,* Ellis Horwood Limited, Chichester.

Rebelo, N., 1991, *Analysis of Rubber Compound with ABAQUS,* Proc. 2nd National Congress of ABAQUS Users' Group Italia, Bologna, Italy.

Renda, V., Verzelletti, G., Gutierrez, E., Magonnette, G., Tirelli, D., Papa, L., and Molina, F. J., 1996, *"Pseudo-Dynamic Tests on Large Scale Models of Base Isolated Structures at the Joint Research Center of the European Commission",* Proc., 1996 ASME-ICVT Pressure Vessel and Piping Conference, Montreal, Quebec, Canada.

Tests required for the implementation of the rubber hyperelastic model in ABAQUS

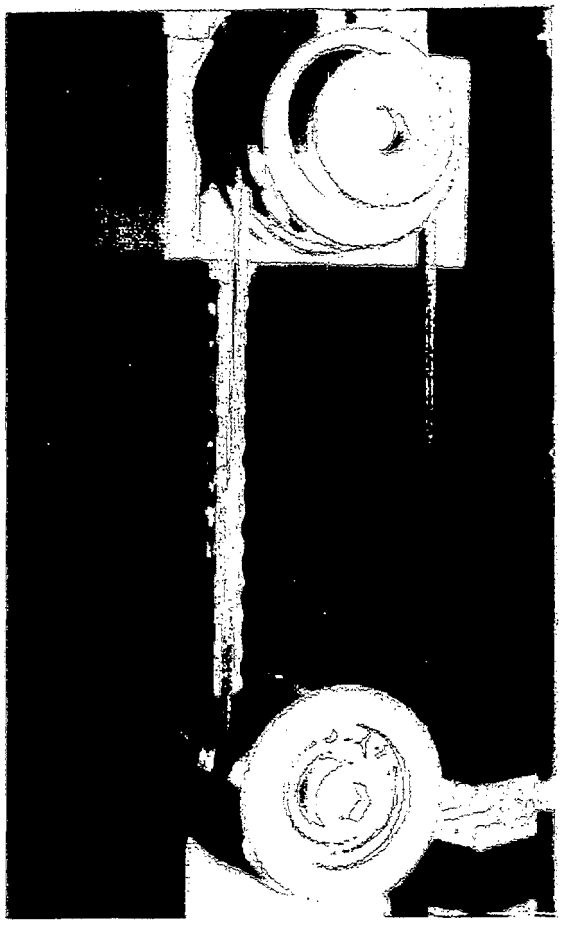

Uniaxial

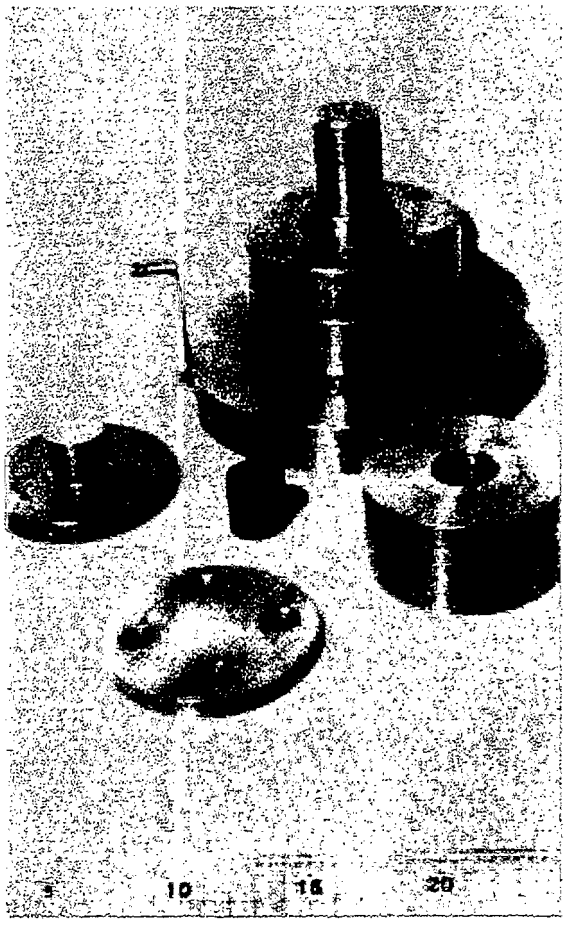

Volumetric

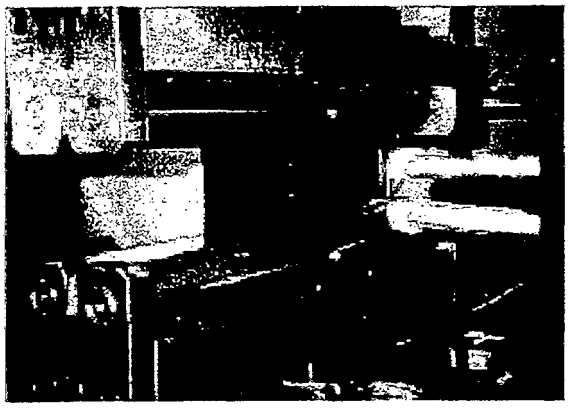

Planar

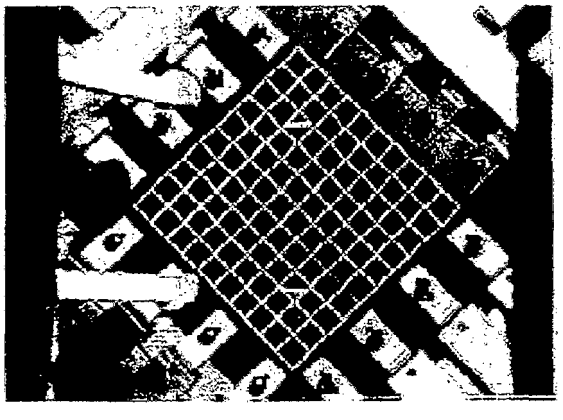

Equibiaxial

Figure 1. Experimental tests on rubber specimens

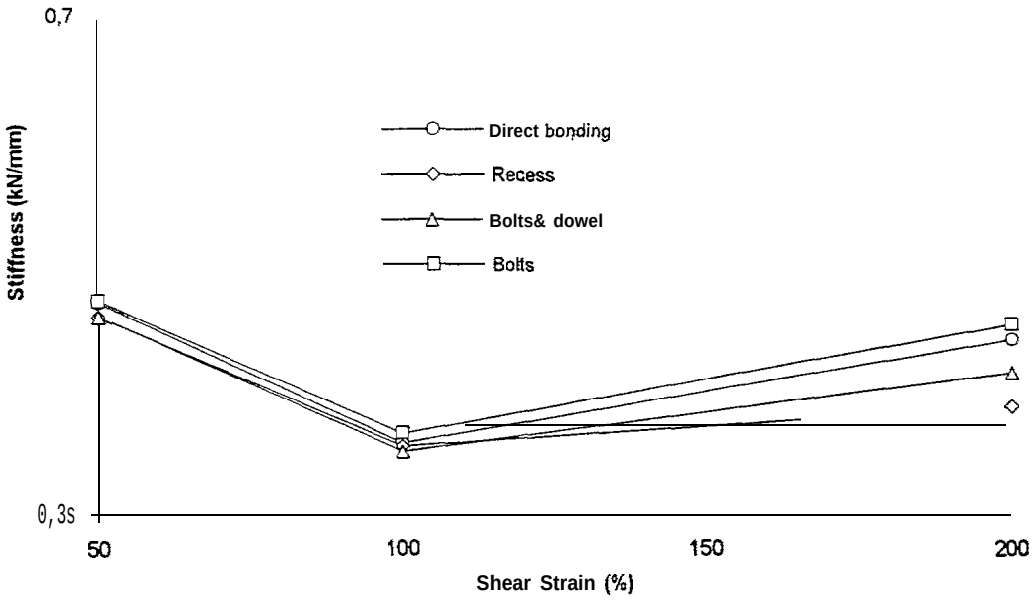

Figure 2. Effects of the attachment system on the static horizontal stiffness for half-scale isolators with low shape factor and hard rubber compound

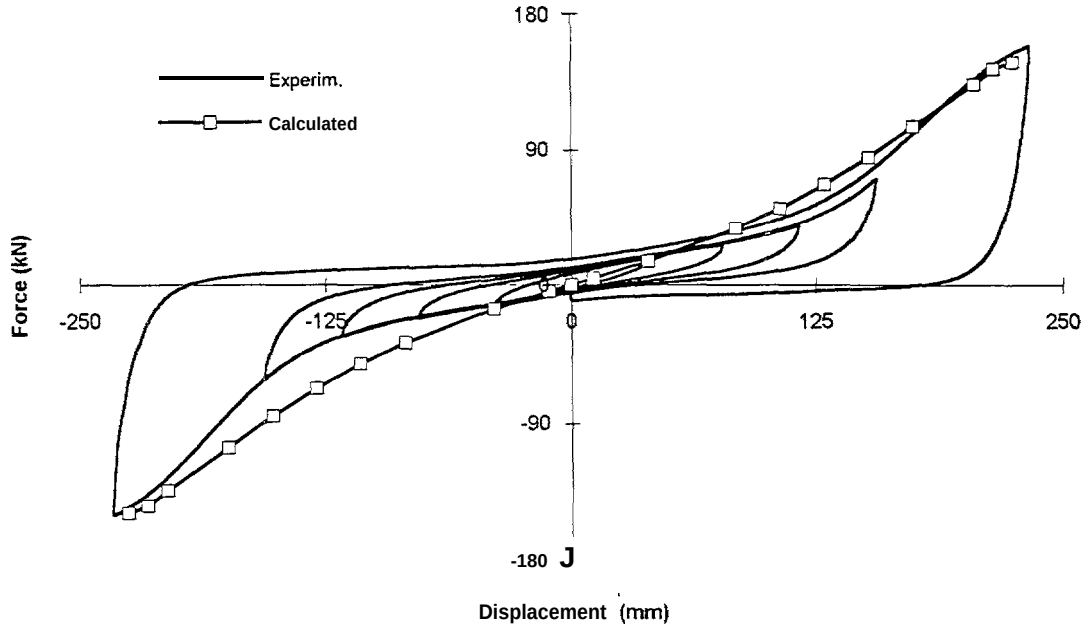

Figure 3. Combined compression and 300% shear strain test on a bolted half-scale isolator with high shape factor and hard rubber compound

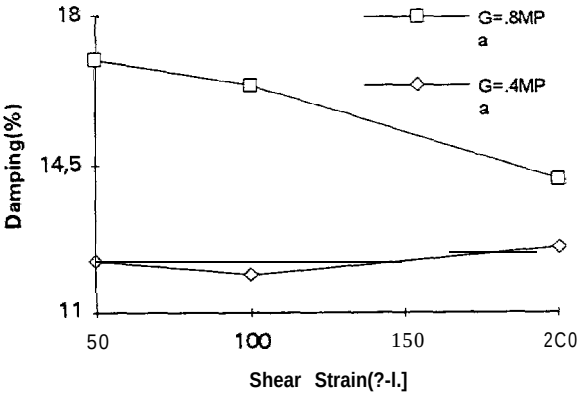

Fig.4. Equivalent viscous damping of the hard and soft rubber compounds in the case of half-scale isolators with low shape factor (quasi-static tests)

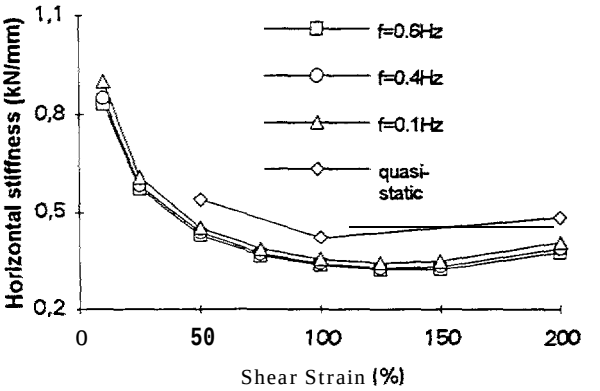

Figure 5. Dynamic and quasi-static horizontal stiffnesses of a bolted half-scale isolator with high shape factor and hard rubber compound

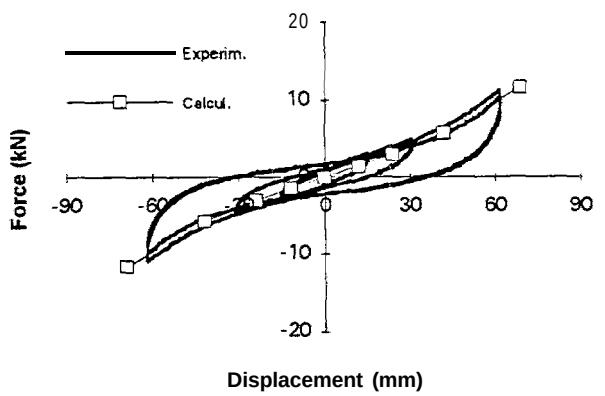

Figure 5-his. Compression (100% design load) & shear (200% shear strain) test on a 'further optimized' isolator (D=125 mm, H=30 mm, S=12,

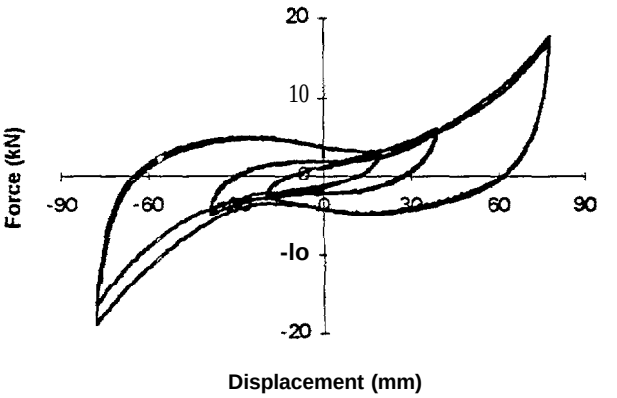

Figure 6. Compression (200% design load) & shear (250% shear strain) test on a 'further optimized' isolator (D=125 mm, H=30 mm, S=12, G=0.4 MPa)

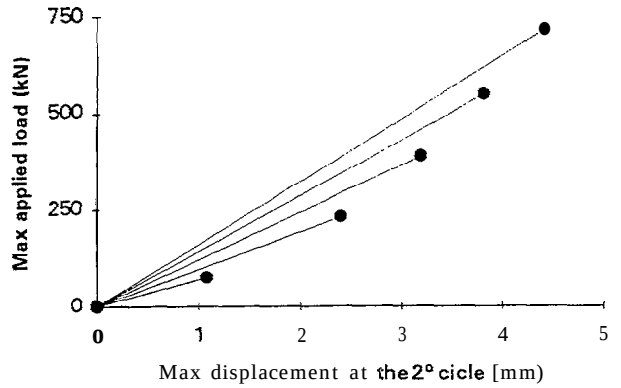

Figure 7. Vertical stiffness of a 'further optimized' isolator (D=125 mm, H=30 mm, S=12, G=0.4 MPa) during compression tests up to 1400% design load

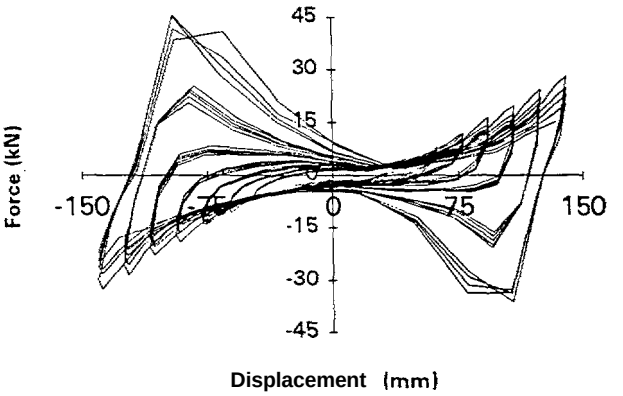

Figure 8. Dynamic (0.1 Hz) horizontal failure test (450% shear strain) on a 'further optimized' isolator (D=125 mm, H=30 mm, S=12, G=0.4 MPa)

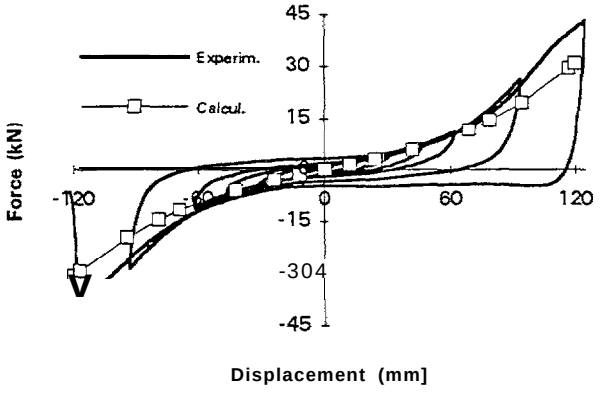

Figure 9. Quasi-static horizontal failure test (400% shear strain) on a 'further optimized' isolator (D=125 mm, H=30 mm, S=12, G=0.4 MPa)

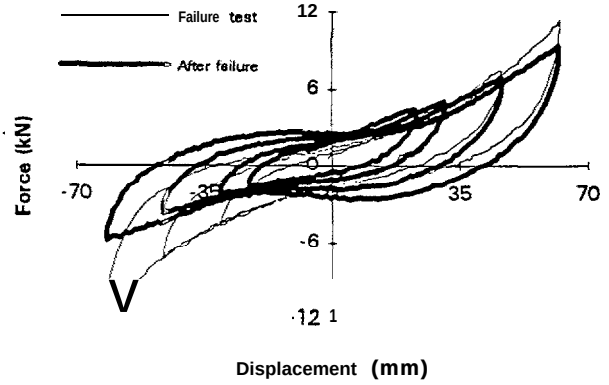

Figure 10. Quasi-static horizontal tests (200% shear strain,) on a 'further optimized' isolator (D=125 mm, H=30 mm, S=12, G=O.4 MPa, same as Fig. 9)

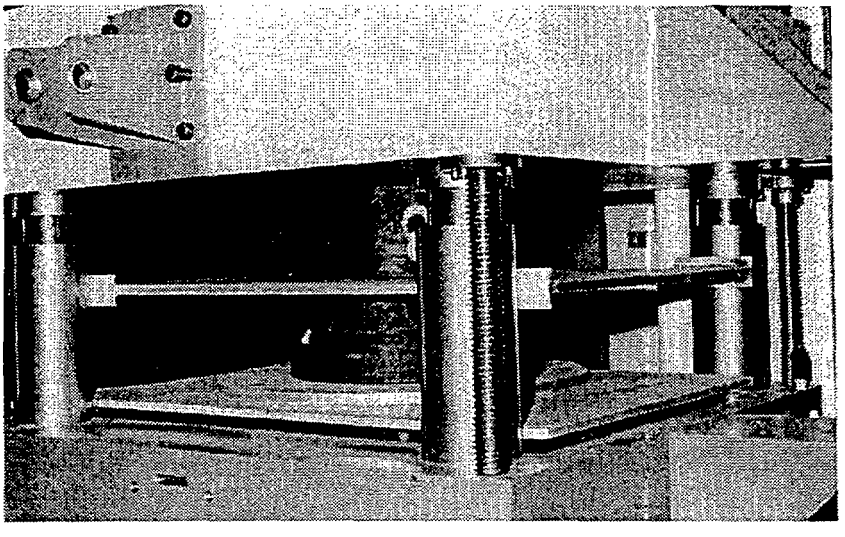

Fig. 11. Isolators during a long period compression test on CAT (Creep & Ageing Test Machine) for the evaluation of the creep effects

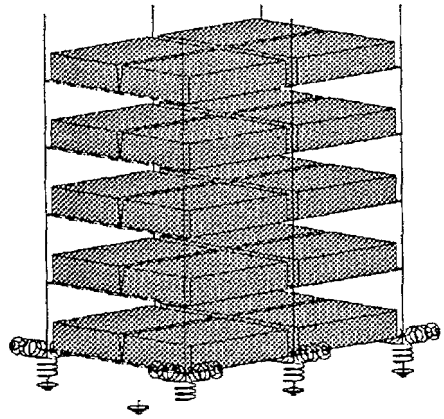

Figure 12. FEM of MISS in the reference configuration (total height = 3.6 m; total weight = 300 kN; isolation frequency= 0.77 Hz)

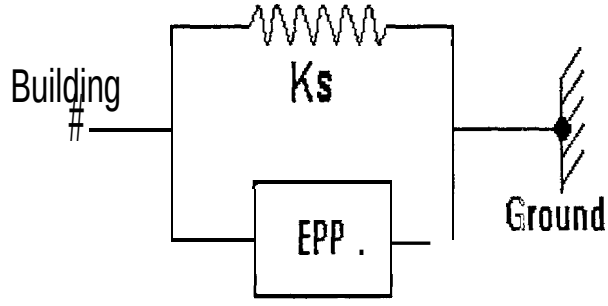

Figure 13-a. Simplified model of seismic isolator: Ks = non-linear spring; EPP = elastic-perfectely plastic beam

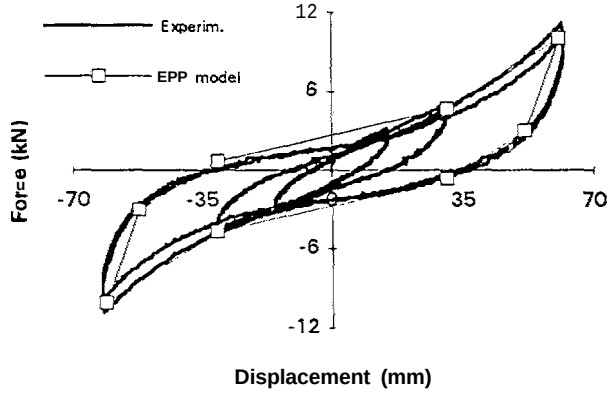

Figure 13-b. Comparison between the experimental & simplified hysteresis loops Of a 'further optimized' isolator- (D=1 25 mm, H=30 mm, S=12, G=0.4 MPa)

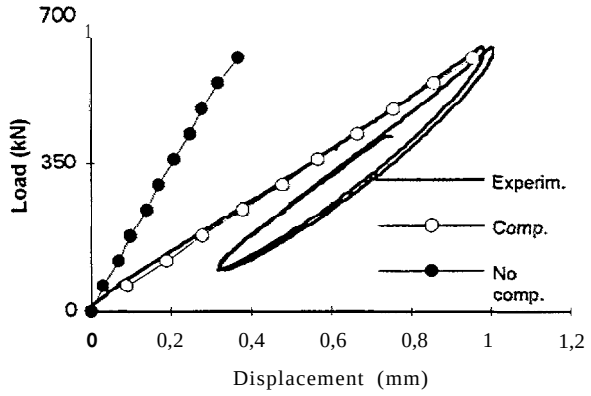

Figure 14. Effects of the compressibility on the calculated vertical stiffness for a bolted isolator with high shape factor and hard rubber compound

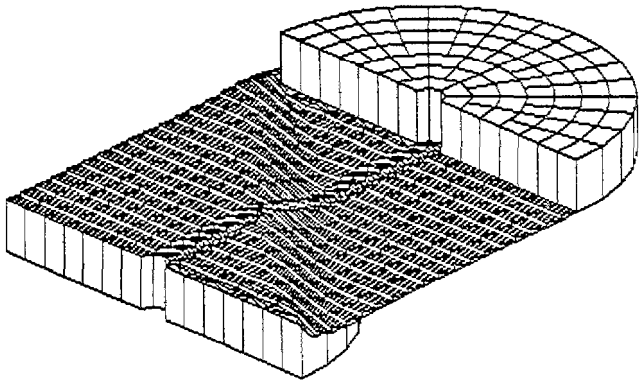

Figure 1 S. FEM of a 'squatter' isolator (D=250 mm, H=45 mm, S=24, G=0. 8 MPa) at S00% shear strain under the design vertical load (400 kN)

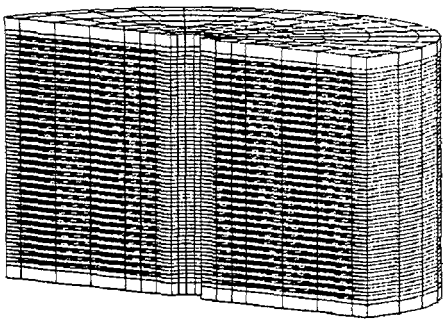

Figure 16-a. FEM of HDRB with symmetry about a vertical axial plane (YSYMM conditions) - Half model

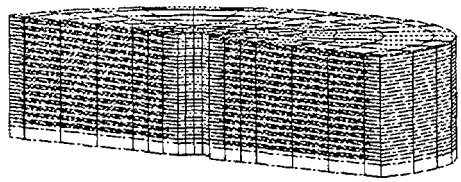

Figure 16-b. FEM of HDRB with symmetry about a vertical axial plane and hemi - simmetry - A Quarter model

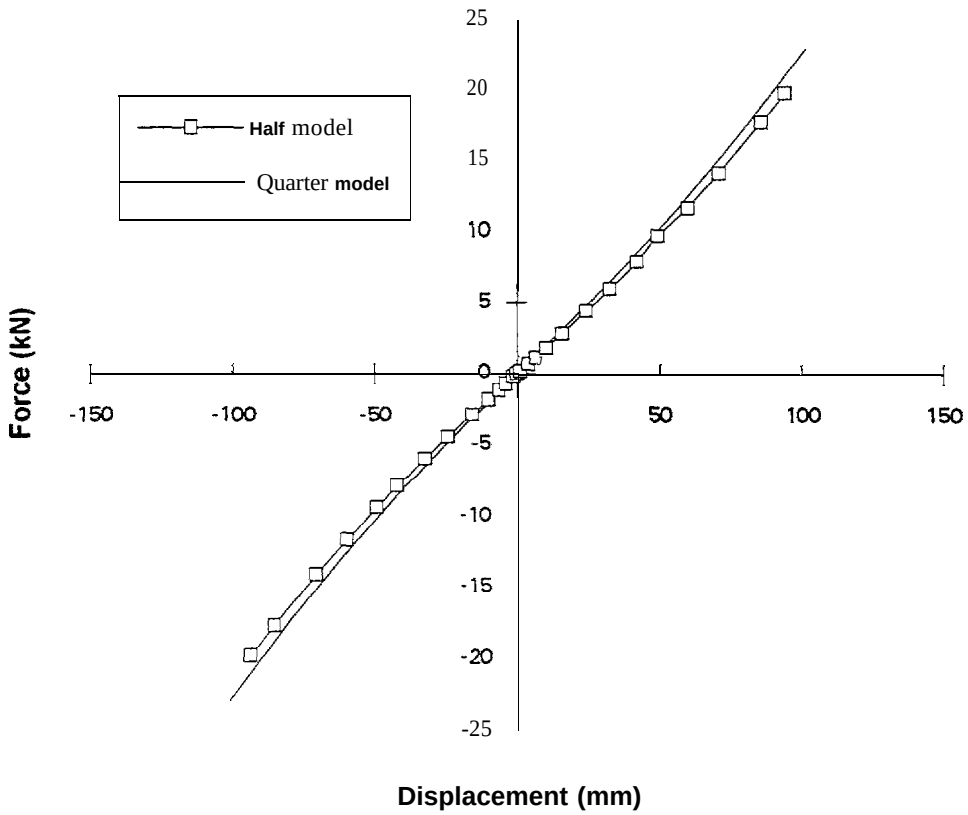

Figure 16-c. Comparison between [he horizontal stiffnesses of HDRB in half scale using the FEMs of figures 5-u and 5-b

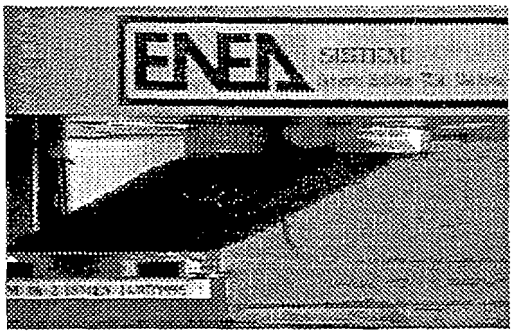

Figure 1 ?-a. Compression and shear test at 300% on a bolted "optimized" HDRB

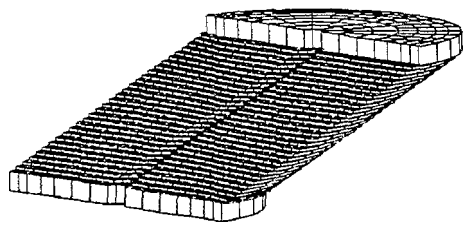

Figure 17-b. FEM of a bolted optimized HDRB at 300 % shear strain

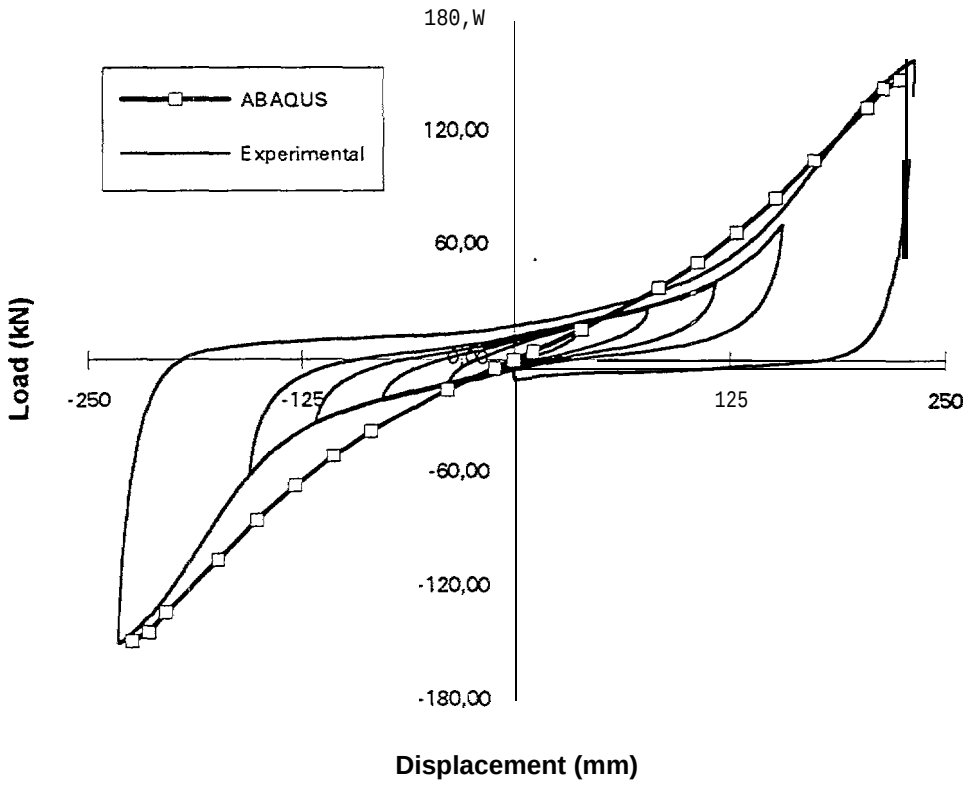

Figure 17-c. Experimental and numerical force-displacement values for a combined compression & 300% shear strain test on a bolted "optimized" HDRB (1:2 scale, diameter=250 mm, H=75 mm, S=24, G= 0.8 MPa)

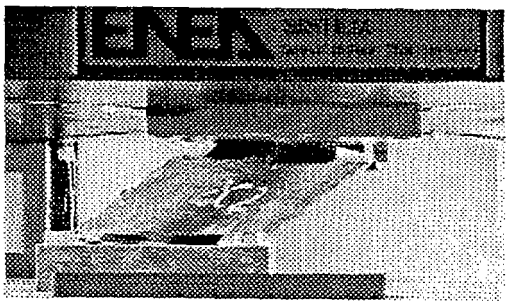

Figure 18-a. Compression and shear test at 200% shear strain on an optimized HDRB with recess attachment system

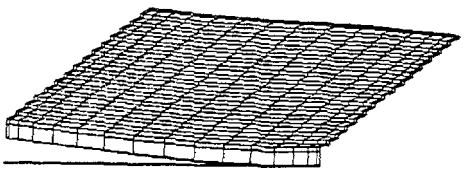

Figure 18-b. A quarter FEM of an optimized HDRB with recess attachment system at 200% shear strain

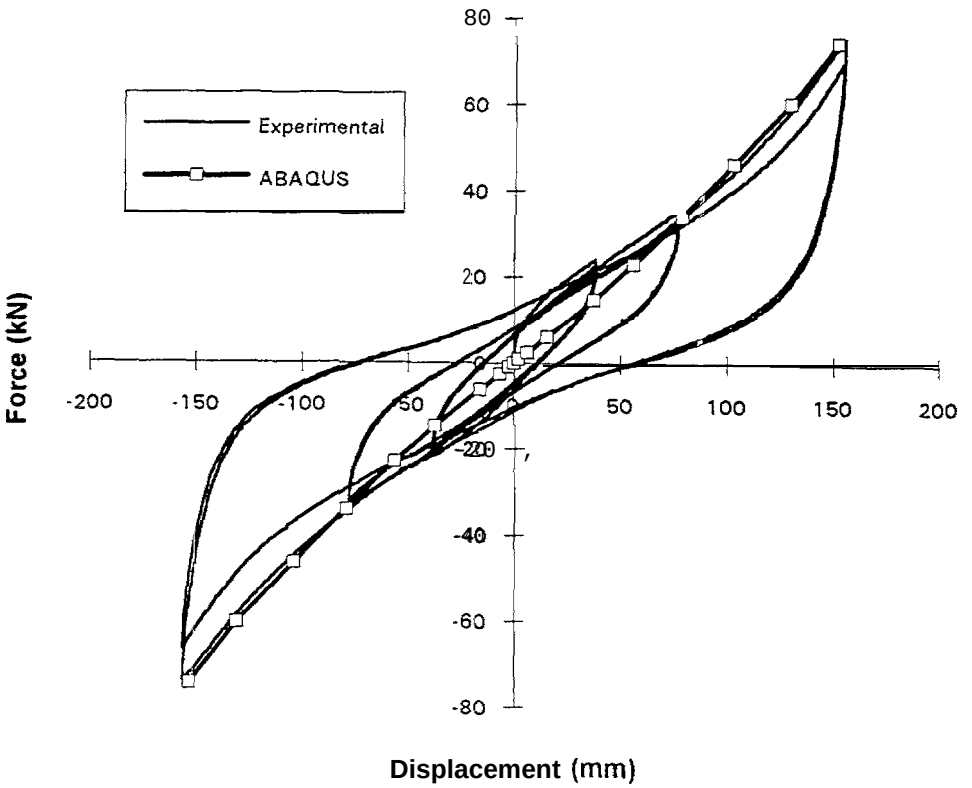

Figure 18-c. Experimental and numerical force-displacement values for a combined compression & 200% shear strain test on an optimized HDRB (1:2 scale, diameter=250 mm, H=75 mm, S=24, G=O. 8 MPa, recess attachment system)

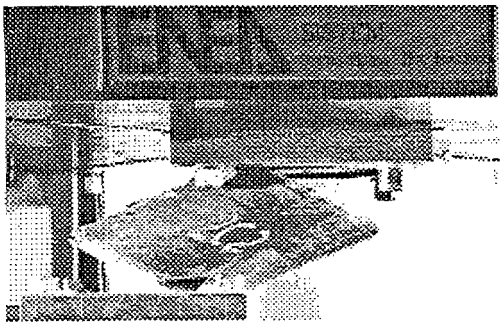

Figure 19-a. Compression and shear test at 300% shear strain on optimized HDRB with recess attachment system

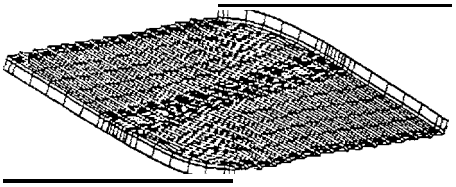

Figure 19-b. FEM of an optimized HDRB at 300% shear strain with recess attachment system

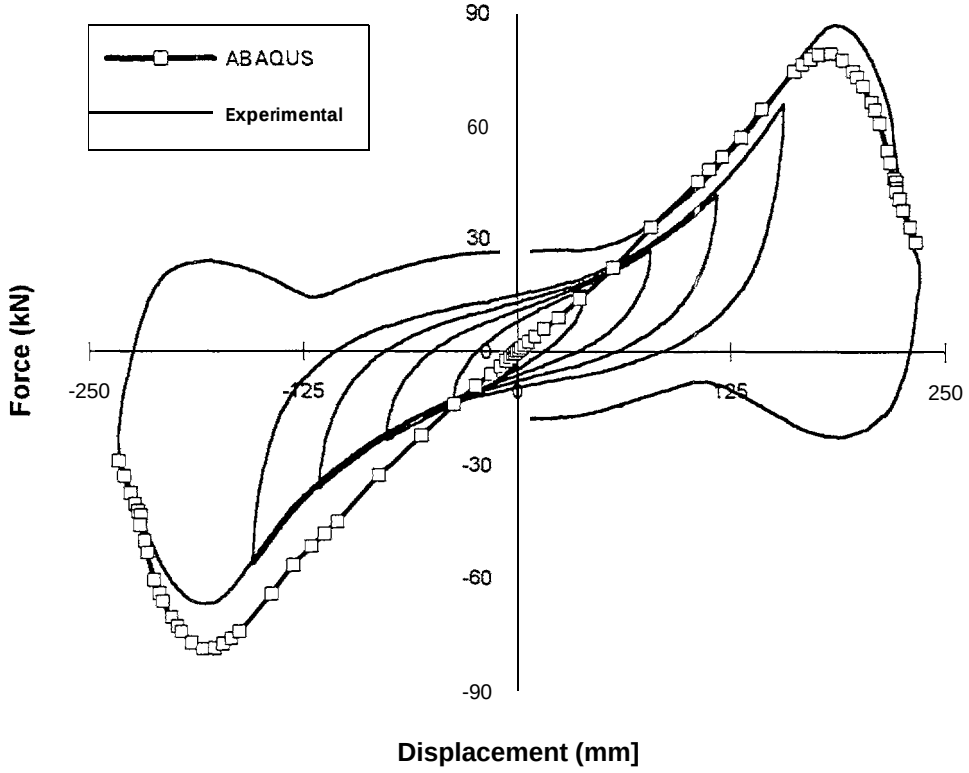

Figure 19-c. Experimental and numerical force-displacement values for a combined compression & 300% shear straintest on optimized HDRB (1:2 scale, diameter= 250 mm, H=75 mm, S=12, G=O. 8 MPa, recess attachment system)

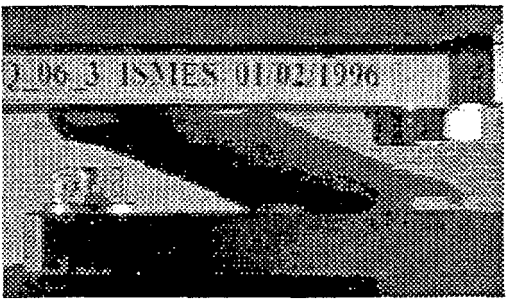

Figure 20-a. Compression and shear test at 400% shear strain on a bolted "futher optimized" HDRB

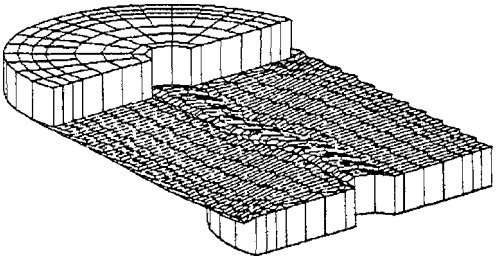

Figure 20-b. FEM of a bolted "further optimized" HDRB at 400% shear strain

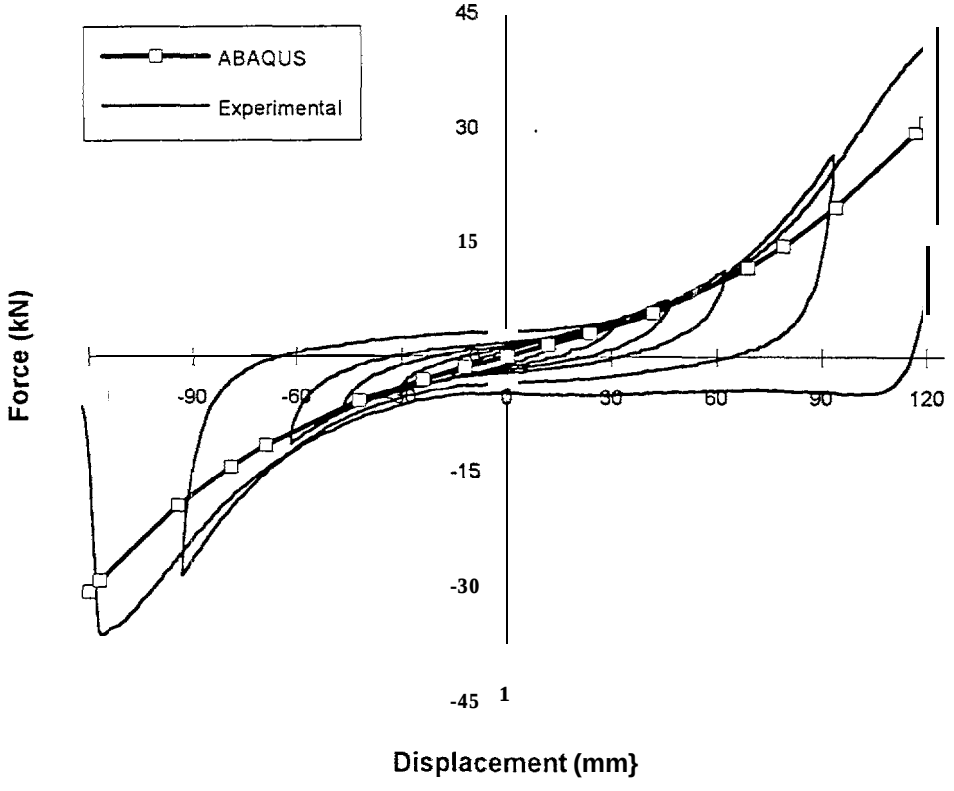

Figure 20-c. Experimental and numerical force-displacement values for a combined compression & 400% shear strain failure test on a bolted "further optimized" HDRB (1:4 scale, diameter=125 mm, H=30 mm, S=12, G=(24 MPa)

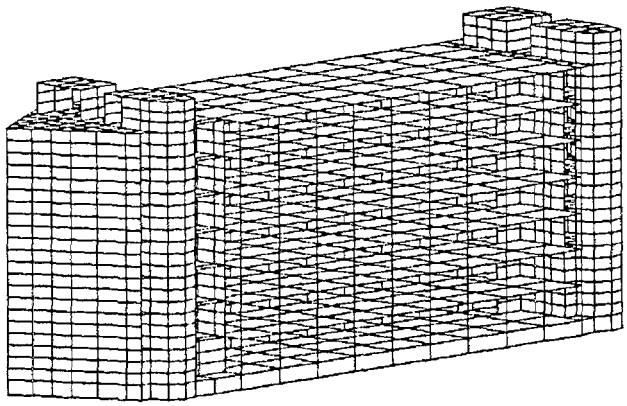

Figure 21. Optimized FEM of the TELECOM Italia building (Ancona) subjected to forced vibrations and pull-back (up to 110 mm) in-situ tests in 1990